# Numerical Simulation of Collisionless Shocks

*Submitted in partial fulfillment of the requirements*

*of*

*Bachelor of Technology Project I*

*by*

Pavan R Hebbar

(*Roll no.* 130010046)


Department of Aerospace Engineering

Indian Institute of Technology Bombay

2015

# B.Tech Project Approval

This B.Tech Project I entitled **"Numerical Simulation of Collisionless Shocks"**, submitted by Pavan R Hebbar(Roll No. 130010046), is evaluated and approved for further continuation as B.Tech Project II in Aerospace Engineering.

**Examiners**

Prof. Upendra V Bandarkar _____

**Supervisors**

Prof. Kowsik Bodi _____

Dr. Bhooshan Paradkar _____

**Date:** ..... November 2015

**Place:** _____

# Declaration of Authorship

I declare that this written submission represents my ideas in my own words and where others' ideas or words have been included, I have adequately cited and referenced the original sources. I also declare that I have adhered to all principles of academic honesty and integrity and have not misrepresented or fabricated or falsified any idea/data/fact/source in my submission. I understand that any violation of the above will be cause for disciplinary action by the Institute and can also evoke penal action from the sources which have thus not been properly cited or from whom proper permission has not been taken when needed.

Signature: .....

**Pavan R Hebbar**

130010046

Date: ..... November 2015

Pavan R Hebbar/ Prof. Kowsik Bodi (Supervisor): **"Numerical Simulation of Collisionless Shocks"**, *B.Tech project I report*, Department of Aerospace Engineering, Indian Institute of Technology Bombay, November 2015.

---

# *Abstract*

We show that collisionless shock waves can be driven in unmagnetized electron-positron plasma by performing a two-dimensional particle-in-cell simulation. At the shock transition region, strong electric and magnetic fields are generated due to Weibel instabilities which exponentially decrease after the transition region. The structure of the shock propagates at an almost constant speed. We show the existence of Weibel like instabilities by observing patterns in the density of thermalized particles. We also analyse the variation of electron-positron densities and their velocities across the shocks.

# Contents

# List of Figures

# Chapter 1

# Introduction

Collisionless shocks are one of the important phenomenas that occur in astronomical plasma. They are believed to be the main source for production of high energy particles like cosmic rays upto $E \sim 10^{17}$ eV. This process of accleration of particles through shocks is called Diffusive Shock Acceleration [1]. In DSA, particles gain energy by repeatedly scattering across the shock, increasing their energy as if being squeezed between two converging walls.

The magnetic and the electric fields are amplified and generated around collisionless shocks in several supernovae remnant. These magnetic fields may be generated by the high-energy particles accelerated at the shocks. For the generation of magnetic fields in the relativistic shocks associated with the afterglows of gamma-ray bursts, Medvedev & Loeb (1999) [2] suggested that the Weibel instability [3] is driven at the shock and generates strong magnetic fields. This mechanism can work in shocks in electron-positron plasmas as well [4].

In this project we would like to study the dynamics of collisionless shocks in unmagnetized electron-positron plasmas in detail by performing a high-resolution two-dimensional particle-in-cell simulation and confirm that a kind of collisionless shock indeed forms, mainly due to the magnetic fields generated by the Weibel-like instability. Over the course of the project we would like to see the variation velocities of individual particles and propose a mechanism for acceleration of the particles.

## 1.1 Motivation

Being an aerospace student, who is also interested in astrophysics, I would like to use my knowledge of fluid flow across shocks in studying collisionless shocks which have astrophysical

implications. Also the knowledge of palsma dynamics that I gain through this project would have various applications in propulsion and other areas of aerospace This has been the main reason for me to chose this project.

## 1.2 Overall Structure

In this report, Chapter 2 deals with the basic desciption of collisionless shocks, Chapter 3 deals with Particle-in-Cell simulations and Chapter 4 deals with the simulation and the results

# Chapter 2

# Basics of Collisionless Shocks

A collisionless shock is loosely defined as a shock wave where the transition from pre-shock to post-shock states occurs on a length scale much smaller than a particle collisional mean free path [5]. The reason such a structure can exist is because particles interact with each other not through Coulomb collisions, but by the emission and absorption of collective excitations of the plasma - plasma waves.

## 2.1 Classification

Collisionless shocks can be classified into various categories based on the direction of magnetic fields before and after shock. Some of the terms used to describe collisionless shocks are:

- **Quasi-perpendicular:** The pre-shock magnetic field is aligned closer to the shock front. In these shocks the particles gyrate back into the shock
- **Quasi-parallel:** The pre-shock magnetic field field vector is aligned closer to the direction of the shock velocity vector. A 1D normal shock is perfectly parallel. In these type of shocks, the particles can get reflected back into the upstream medium.
- **Slow mode:** The magnetic field along the shock front decreases on going through the shock. They require $v_{shock}/v_{sound} > 1$ but an Alfven Mach number of $v_{shock}/v_{alfven} < 1$ i.e magnetic energy density > gas pressure in the upstream medium.
- **Fast mode:** The magnetic field along shock front increases on going through the shock. Fast mode shocks require $v_{shock}/v_{Alfven} > 1$ in parallel propagation & $v_{shock}/\sqrt{v_{Alfven}^2 + v_{sound}^2} > 1$ in perpendicular propagation.

- **Unmagnetized Shocks:** Besides the above kinds of shocks in which there exists a magnetic field upstream, shocks can even form in unmagnetized plasma. In this project, we mainly focus on these kinds of shocks.

## 2.2 Weibel Instability

The Weibel instability is a plasma instability present in homogeneous or nearly homogeneous electromagnetic plasmas which possess an anisotropy in momentum (velocity) space [6]. This anisotropy is most generally understood as two temperatures in different directions. Burton Fried(1959) [7] showed that this instability can be understood more simply as the superposition of many counter-streaming beams. It is like the two-stream instability except that the perturbations are electromagnetic and result in filamentation as opposed to electrostatic perturbations which would result in charge bunching. In the linear limit the instability causes exponential growth of electromagnetic fields in the plasma which help restore momentum space isotropy.

As an example, to understand the formation of unmagnetized shock, consider the following non relativistic case:

An electron beam with density $n_{b0}$ and initial velocity $v_0\mathbf{z}$ propagating in a plasma of density $n_{p0} = n_{b0}$ with velocity $-v_0\mathbf{z}$. SInce there is no background electromagnetic field, $\mathbf{B_0} = \mathbf{E_0} = 0$. The perturbation will be taken as an electromagnetic wave propagating along $\hat{\mathbf{x}}$ i.e. $\mathbf{k} = k\hat{\mathbf{x}}$. Assume the electric field has the form:

$$\mathbf{E_1} = Ae^{i(kx-\omega t)}\mathbf{z} \tag{2.1}$$

From Faraday's laws we obtain:

$$\nabla \times \mathbf{E_1} = -\frac{\partial \mathbf{B_1}}{\partial t} \Rightarrow i\mathbf{k} \times \mathbf{E_1} = i\omega \mathbf{B_1} \Rightarrow \mathbf{B_1} = \hat{\mathbf{y}}\frac{k}{\omega}E_1 \tag{2.2}$$

Since the perturbations are small, we can linearise the velocity of electron beam by writing $\mathbf{v_b} = \mathbf{v_{b0}} + \mathbf{v_{b1}}$ and density $n_b = nb0 + nb1$. Assuming $\mathbf{v_{b0}}$ and $n_{b0}$ to be constant, and the perturbation velocities to be very small, we apply the Newton-Lorentz equation and simplify to get

$$-i\omega m\mathbf{v_{b1}} = -e\mathbf{E_1} - e\mathbf{v_{b0}} \times \mathbf{B_1} \tag{2.3}$$

Decomposing the equation into components we get:

$$v_{b1z} = \frac{eE_1}{mi\omega} \qquad v_{b1x} = \frac{eE_1}{mi\omega}\frac{kv_{b0}}{\omega} \tag{2.4}$$

We use the continuity equations to find the perturbation density:

$$\frac{\partial n_b}{\partial t} + \nabla \cdot (n_b \mathbf{v_b}) = 0 \tag{2.5}$$

simplitfying we get:

$$n_{b1} = n_{b0}\frac{k}{\omega}v_{b1x} \tag{2.6}$$

Now we use the equation of current density of beam to get:

$$J_{b1x} = -n_{b0}e^2E_1\frac{kv_{b0}}{im\omega^2} \qquad J_{b1z} = -n_{b0}e^2E_1\frac{1}{im\omega}(1 + \frac{k^2v_{b0}^2}{\omega^2}) \tag{2.7}$$

Doing a similiar analysis for plasma, it can be seen that the x components of current densities of electron beam and plasm cancel each other while the z components get added. Thus:

$$\mathbf{J_1} = -2n_{b0}e^2E_1\frac{1}{im\omega}(1 + \frac{k^2v_{b0}^2}{\omega^2})\hat{\mathbf{z}} \tag{2.8}$$

Substituting in Maxwell's equations nd manipulating we get,

$$\mathbf{E_1} = A\hat{\mathbf{z}}e^{\gamma t}e^{ikx} \tag{2.9}$$

$$\mathbf{B_1} = \hat{\mathbf{y}}\frac{k}{\omega}E_1 = \hat{\mathbf{y}}\frac{k}{i\gamma}Ae^{\gamma t}e^{ikx} \tag{2.10}$$

where: $\gamma = \frac{\omega_p k v_0}{(\omega_p^2+k^2c^2)^{1/2}} = \omega_p\frac{v_0}{c}\frac{1}{(1+\frac{\omega_p^2}{k^2c^2})^{1/2}}$ It can be seen that,

$$\frac{|B_1|}{|E_1|} = \frac{k}{\gamma} \propto \frac{c}{v_0} >> 1 \tag{2.11}$$

These Weibel instabilities have a length scale of $c/\omega_p$ and time scales of $10/\omega_p$. As the two current filaments merge, the field cascades from $c/\omega_p$ to larger scales, thus increasing the magnitude of electric and magnetic fields produced. Once the electromagnetic fields reach a certain value, they can deflect the particles leading to collisionless shocks.

# Chapter 3

# Particle-in-Cell Simulations

The idea of the PIC simulation is simple: The code simulates the motion of plasma particles and calculates all macro-quantities (like density, current density and so on) from the position and velocity of these particles. The macro-force acting on the particles is calculated from the field equations. The name "Particle-in-Cell" comes from the way of assigning macro-quantities to the simulation particles. In general, any numerical simulation model, which simultaneously solves equations of motion of N particles

$$\frac{d\mathbf{X_i}}{dt} = \mathbf{V_i} \qquad , \qquad \frac{d\mathbf{V_i}}{dt} = \mathbf{F_i}(t, \mathbf{X_i}, \mathbf{V_i}, A) \tag{3.1}$$

for $i = 1, ..., N$ and of macro fields $A = L1(B)$, with the prescribed rule of calculation of macro quantities $B = L2(X1, V1, ..., XN, VN)$ from the particle position and velocity can be called a PIC simulation. For plasma simulations PIC codes are usually associated with codes solving the equation of motion of particles with the Newton-Lorentz's force(changed according to relativistic formulas)

$$\frac{d\mathbf{X_i}}{dt} = \mathbf{V_i} \quad , \quad \frac{\gamma}{c}\frac{d\mathbf{V_i}}{dt} = \frac{q}{mc}\left(E + \frac{u \times B}{\gamma}\right) \tag{3.2}$$

for $i = 1, ...., N$ and the Maxwell equation

$$\begin{aligned} \nabla \cdot \mathbf{D} = \rho(\mathbf{r}, t) \qquad & \frac{\partial \mathbf{B}}{\partial t} = -\nabla \times \mathbf{E} \qquad \mathbf{D} = \epsilon \mathbf{E} \\ \nabla \cdot \mathbf{B} = 0 \qquad & \frac{\partial \mathbf{D}}{\partial t} = \nabla \times \mathbf{H} - \mathbf{J}(\mathbf{r}, t) \qquad \mathbf{B} = \mu \mathbf{H} \end{aligned} \tag{3.3}$$

## 3.1 Particle Movers

During PIC simulation the trajectory of all particles is followed, which requires solution of the equations of motion for each of them. This part of the code is frequently called "particle mover" The number of particles in real plasma is extremely large and exceeds by orders of magnitude a maximum possible number of particles, which can be handled by the best supercomputers. Hence, during a PIC simulation it is usually assumed that one simulation particle consists of many physical particles. Because the ratio charge/mass is invariant to this transformation, this superparticle follows the same trajectory as the corresponding plasma particle.
The time in PIC is divided into discrete time moments. Usually the time step, $\Delta t$, between the nearest time moments is constant. Thus: $t \to t_k = t_0 + k\Delta t$ and $A(t) \to A_k = A(t = t_k)$

### 3.1.1 Leap - frog method

The leap-frog method calculates particle velocity not at usual time steps $t_k$ , but between them $t_{k+1/2} = t_0+(k+1/2)\Delta t$. In this way equations become time centred, so that they are sufficiently accurate and require relatively short calculation time. It is an explicit time solver in that in depends only on older values from previous time steps

$$\begin{aligned} \frac{\mathbf{X}_{k+1} - \mathbf{X}_k}{\Delta t} &= \mathbf{V}_{k+1/2}, \\ \frac{\mathbf{V}_{k+1/2} - \mathbf{V}_{k-1/2}}{\Delta t} &= \frac{e}{m}\left(\mathbf{E}_k + \frac{\mathbf{V}_{k+1/2} - \mathbf{V}_{k-1/2}}{2} \times \mathbf{B}_k\right) \end{aligned} \tag{3.4}$$

### 3.1.2 Boris method

This method is frequently used is PIC simulations. Here we write

$$\mathbf{X}_{k+1} = \mathbf{X}_k + \Delta t \mathbf{V}_{k+1/2} \qquad \mathbf{V}_{k+1} = \mathbf{u}_+ + q\mathbf{E}_k \tag{3.5}$$

where $\mathbf{u}_+ = \mathbf{u}_- + (\mathbf{u}_- + (\mathbf{u}_- \times \mathbf{h})) \times \mathbf{s}$, $\mathbf{u}_- = \mathbf{V}_{k-1/2} + q\mathbf{E}_k$, $\mathbf{h} = q\mathbf{B}_k$, $\mathbf{s} = 2\mathbf{h}/(1 + h^2)$ and $q = \Delta t/(2(e/m))$. In general, the Boris method requires 39 operations (18 adds and 21 multiplies).

## 3.2 Boundary Effects

Physically, particles can be absorbed at boundaries, or injected from there with any distribution. But, numerical implentation leads to problems like (i) the velocity and position of particles are shifted in time ($\Delta t/2$), and (ii) the velocity of particles are known at discrete time steps, while a particle can cross the boundary at any moment between these steps. Here we discuss how different boundary conditions are implemented in PIC simulations.

- **Reflection:** One of the frequently used reflection model is specular reflection. Here, $X_{k+1}^{refl} = -X_{k+1}$ and $V_{k+1/2}^{x,refl} = -V_{k+1/2}^{x}$. It is the simplest reflection model, but the accuracy is very low.

- **Reinjection:** Reinjection is applied usually when the fields satisfy periodic boundary. The reinjection is given by $X_{k+1}^{refl} = L - X_{k+1}$ and $V_{k+1/2}^{x,refl} = V_{k+1/2}^{x}$ where $x = L$ denotes the opposite boundary.If the fields are not periodic, then this expression has to be modified. Otherwise a significant numerical error can arise.

- **Absorption:** particle absorption is the most trivial operation and done by re-moving of the particle from memory.

- **Injection:** When a new particle is injected it has to be taken into account that the initial coordinate and velocity are known at the same time, while the leap-frog scheme uses a time shifted values of them. In most cases the number of particles injected per time step is much smaller than the number of particles near the boundary, hence, the PIC code use simple injection models.

# Chapter 4

# Simulation and Results

## 4.1 Simulation Setup

We use WARP open-source code [8] for the simulation of collisionless shocks. WARP is a fully relativistic code that takes input and gives output in Python interface but processes the data in FORTRAN. Here we have performed simulation of electron-positron plasma with two spatial and three velocity dimensions (2D3V).

From now on we use $\tau = \omega_{pe,0}^{-1}$ as the unit of time and the electron skin depth $l_0 = c\omega_{pe,0}^{-1}$ as the unit of length, where $\omega_{pe,0} = (4\pi n_{e0} e^2/m_e)^{1/2}$ is the electron plasma frequency. The units of electric and magnetic fields are both taken as $E_* = B_* = c(4\pi n_{e0} m_e)^{1/2}$ ; they are defined so that their corresponding energy densities are both equivalent to half of the mean electron rest mass energy density.

The simulations were performed on a $N_z \times N_x = 6400 \times 128$ grid, with 80 particles per cell for both species. The complete simulation box is of $L_z \times L_x = 640 \times 15$ in the units of $l_0$. Thus $(\Delta z, \Delta x) = (0.1, 0.1)$. The time step is taken as $\Delta t = 0.04$

Since we consider collisionless shocks in unmagnetized plasmas, the electromagnetic fields were initially set to zero over the entire simulation box. The boundary condition of the electromagnetic field is periodic in each direction.

In this simulation, collisionless shock is formed by merger of 2 high-speed plasma flows with velocities in opposite directions. The two walls at $z = 0$ and $z = 640$ are absorbing for both particles and fields. Initially each plasma flow is loaded uniformly in half the simulation box. The plasma between $z = 0$ and $z = 320$ are given a bulk velocity of $u_z = 2.0$ while the particles between $z = 320$ and $z = 640$ are given a bulk velocity of $u_z = -2.0$(both corresponding to

bulk Lorentz factor $\Gamma = 2.24$) . Their thermal velocities were given so that the distribution of each component of the 4-velocity $u_i (i = x, y, z)$ obeys a Gaussian distribution with a standard deviation of $\sigma_{th} = 0.1$ in the plasma rest frame. At initial stages of the simulation, particles of the two flows near $z = 320$ interact as the two flows merge. This interaction causes some instabilities, and then two collisionless shocks are formed progating in opposite directions

## 4.2 Results

All the above results refer to $4000^{th}$ iteration unless specified.

Figure 4.1 shows the electron number density,$n_e$ across the simulation box. The middle region is the region of shock. We observe that the number density rapidly increases while crossing the transition regions,i.e from $z = 190$ to $z = 260$ and $z = 380$ to $z = 450$, and then it becomes homogeneous. The transition regions do not have a one-dimensional structure, but rather a two-dimensional filamentary structure, with density fluctuations along the y-direction. The typical size of the filaments is on the order of several electron skin depths.

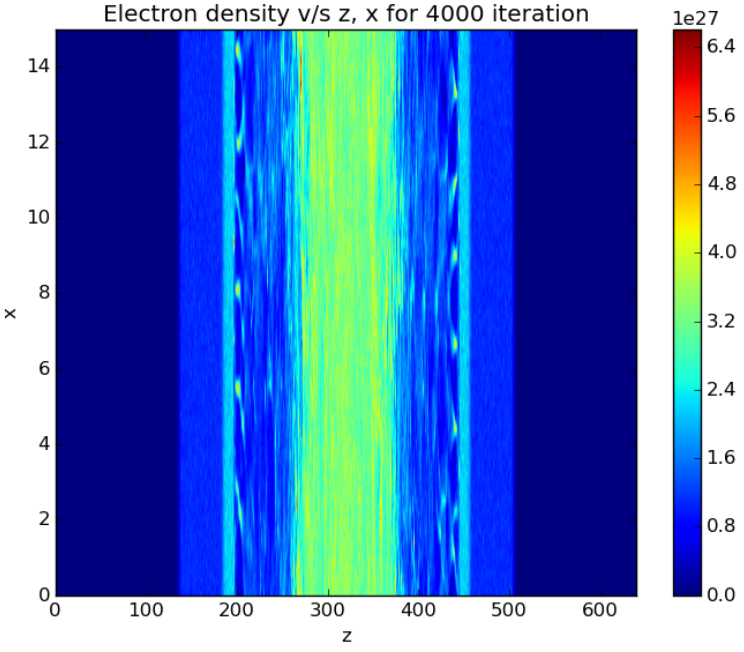


Figure 4.1: Density variation across the grid

Figure 4.2 shows the time development of the electron number density. The horizontal and vertical axes represent the z-coordinate and time, respectively. The plotted number density is

averaged over the y-direction. We observe that the transition region, which is visible as the jump in the number density, propagates upstream with time at an almost constant speed.The thin structure propagating upstream at almost the speed of light is due to particles that have passed at very early stages of simulation when the shock hadn't formed. This structure fades as time passes and won't be seen at later time steps.

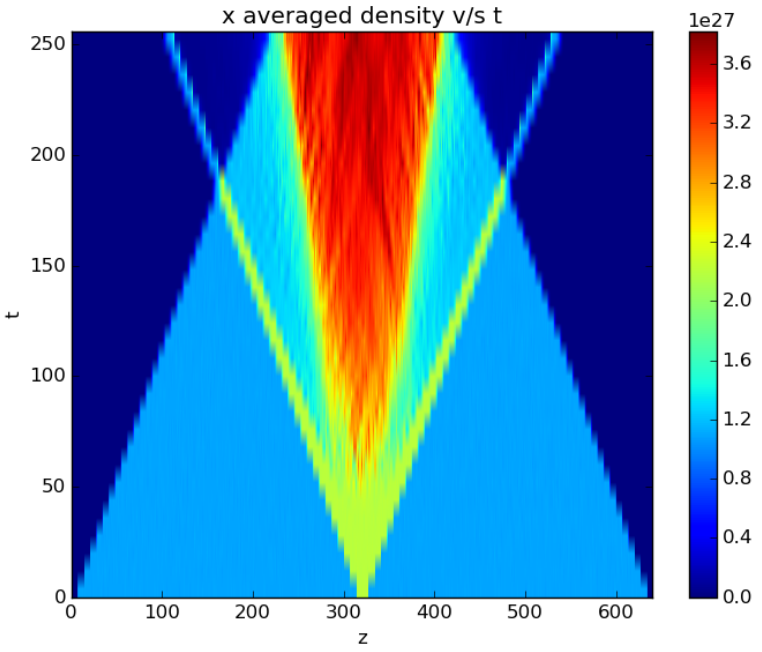


Figure 4.2: Density variation with time

Figure 4.3 shows the x -averaged profiles across the simulation box, normaised to the upstream value. We see that there is an initial increase in density at the point beginning of the transition regions. The two shocks propagate in opposite directions, implying that the region of shock in between keeps increasing with passage of time. The compression ratio across the shocks is 3.3.

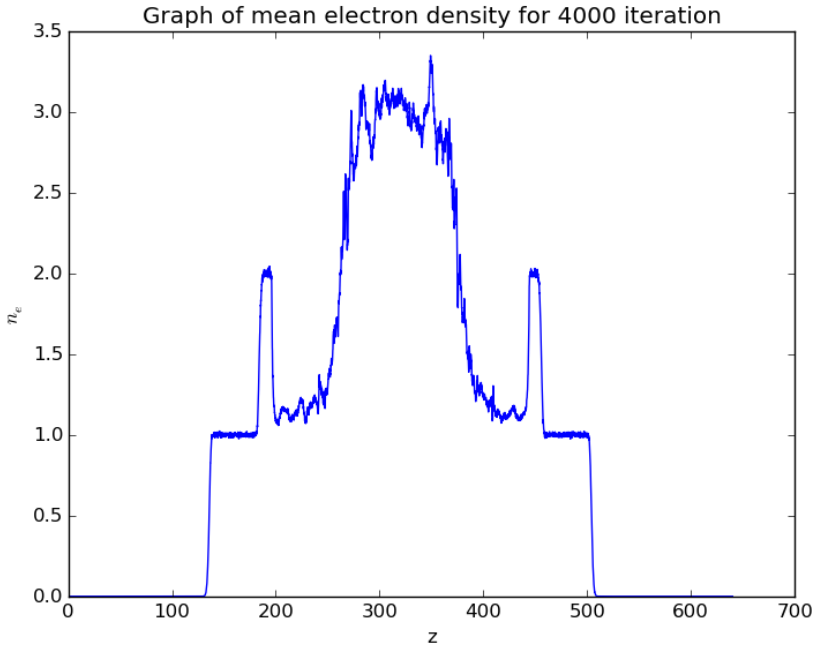


Figure 4.3: Electron density averaged wrt x v/s z

Figure 4.4 and 4.5 represents the x - averaged profiles of electric and magnetic fields across simulation box. We see the presence of strong electric and magnetic fields that increase exponentially in the transition region and then decay in the region of shock.

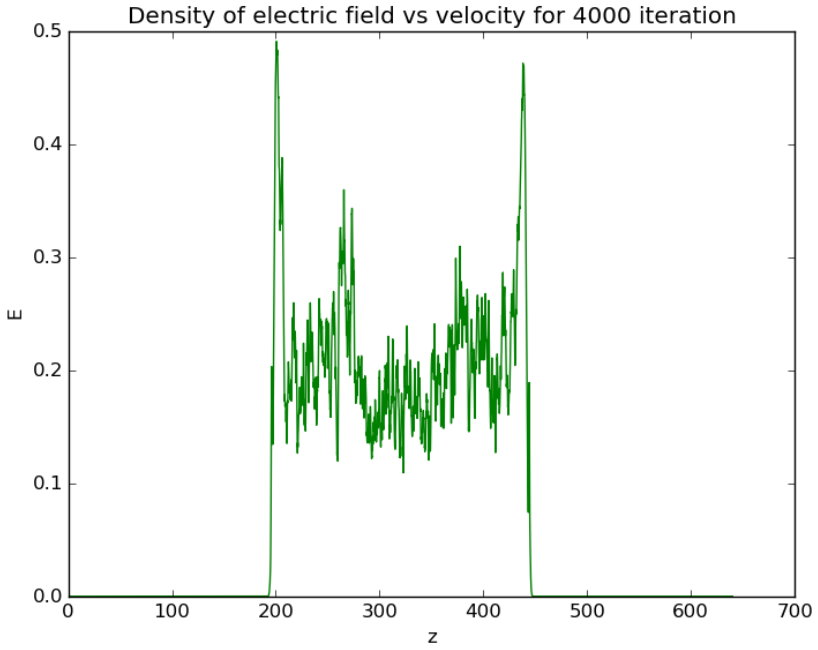


Figure 4.4: x-averaged electric fields v/s z

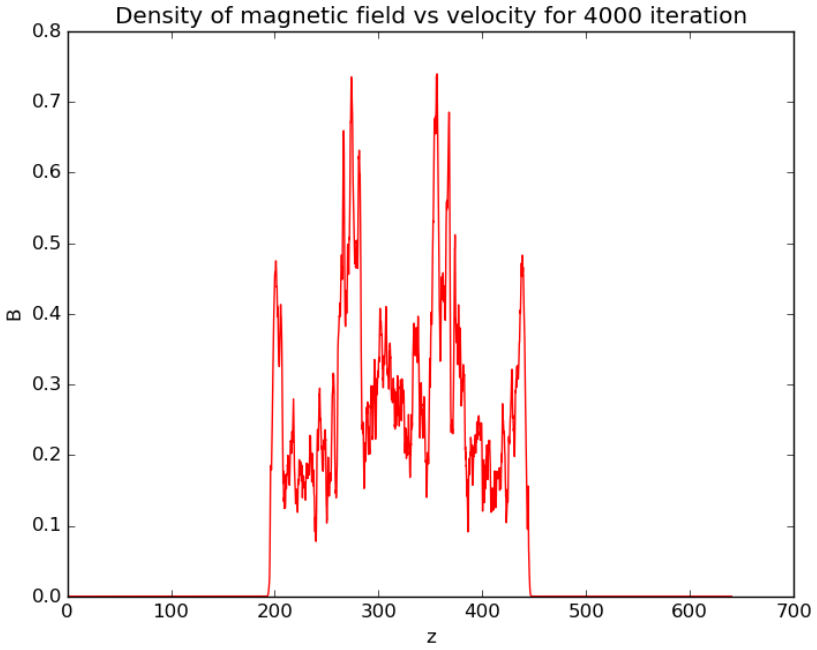


Figure 4.5: x-averaged magnetic fields v/s z

Figure 4.6 shows the distribution of magnetic field across x and z axes at 1200 iteration. In this figure we can see the sinusoidal variation of magnetic field in X direction. This shows the onset of Weibel instabilities that lead to the formation of the shock.

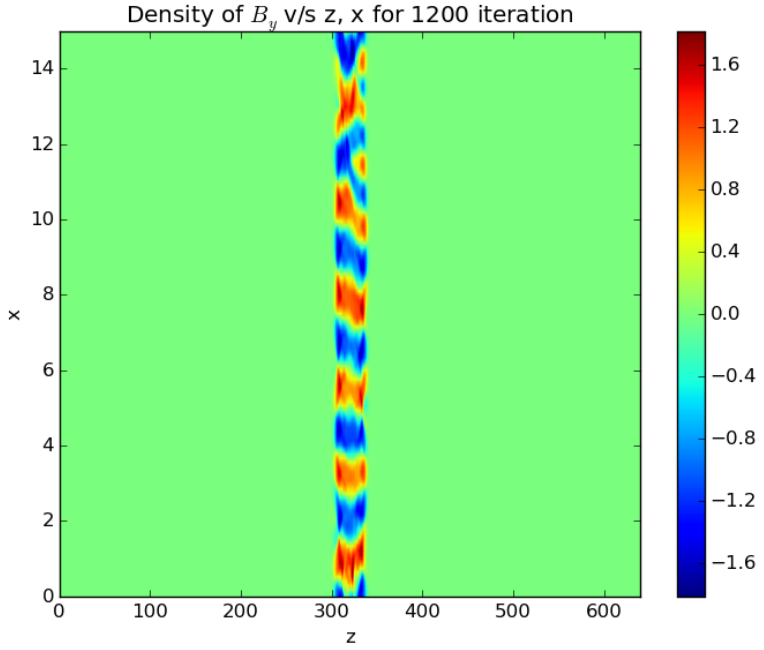


Figure 4.6: Onset of Weibel instabilities

We also look at the variation in the velocity distribution with time. We see that initially the velocities of the two flows are seperate, but as the simulation progresses we see that the velocities tend to merge and they also tend more and more particles reach higher velocities. This can be seen in the following figures

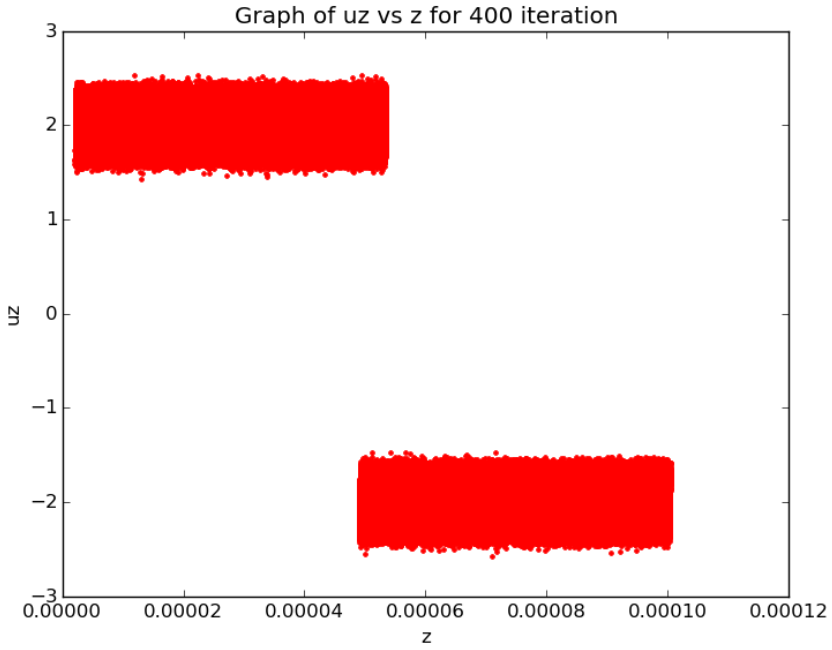


Figure 4.7: uz v/s z for 400th iteration

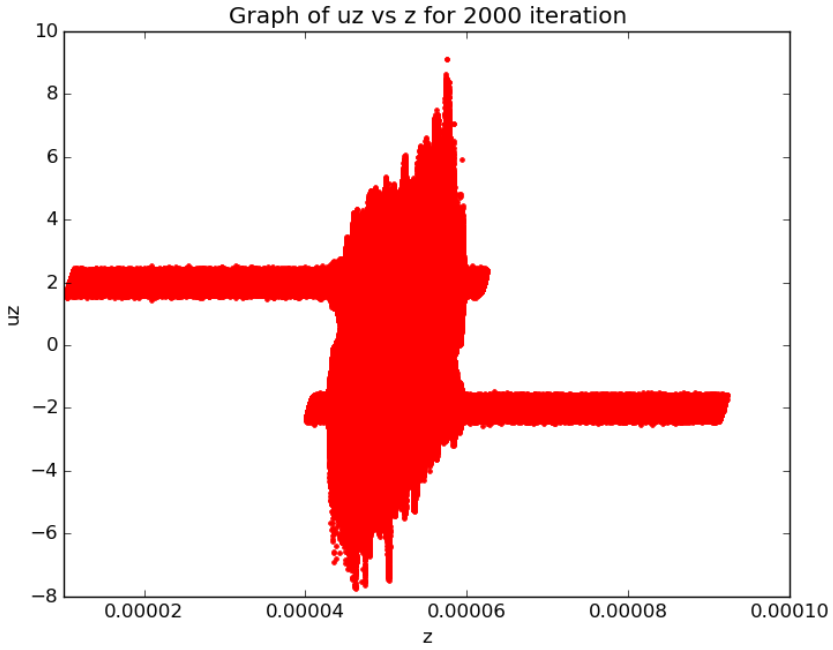


Figure 4.8: uz v/s z for 2000th iteration

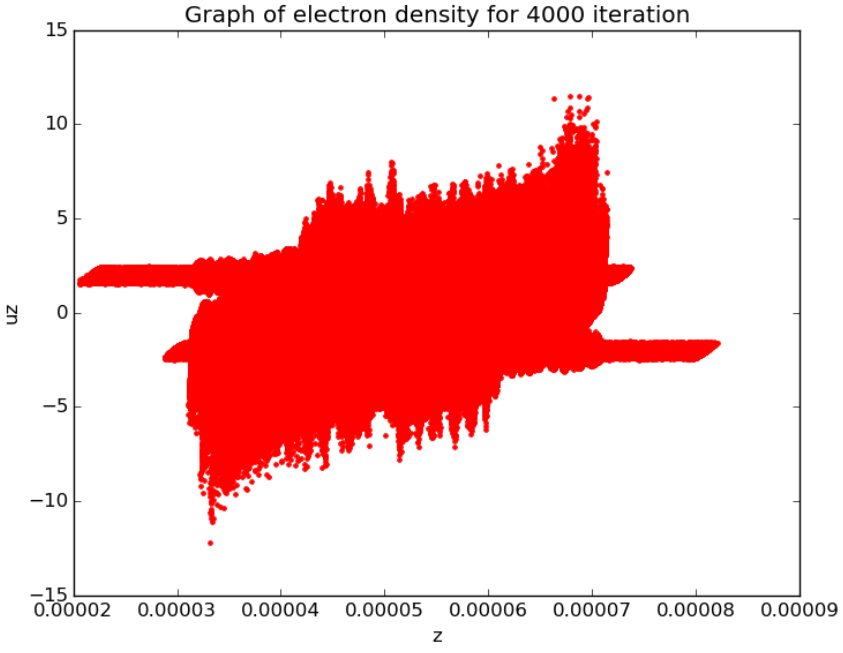


Figure 4.9: uz v/s z for 4000th iteration

40

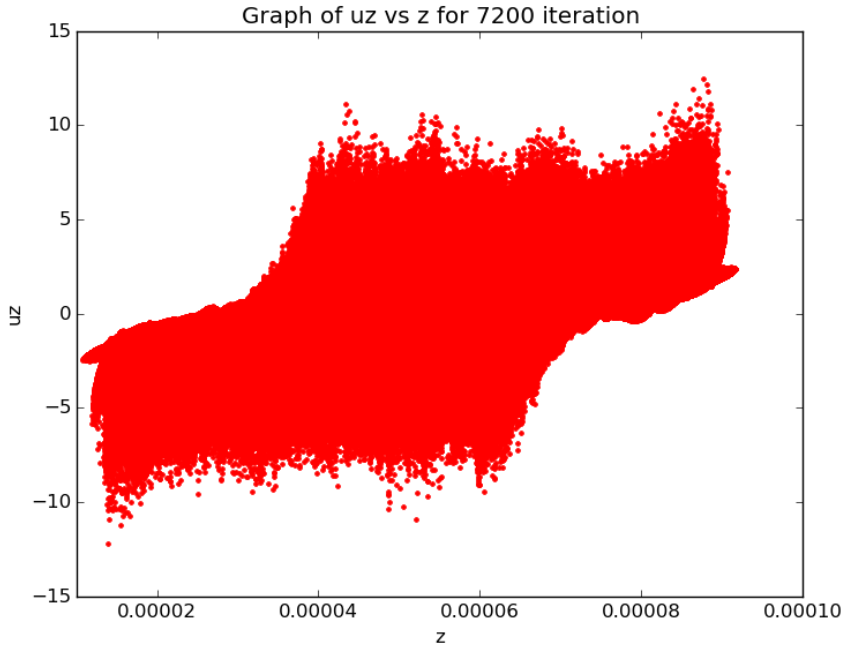


Figure 4.10: uz v/s z for 7200th iteration

Fig 4.11 shows the variation of maximum uz with time.Note that the highest velocity reached is around 10, after which the maximum uz is almost constant.

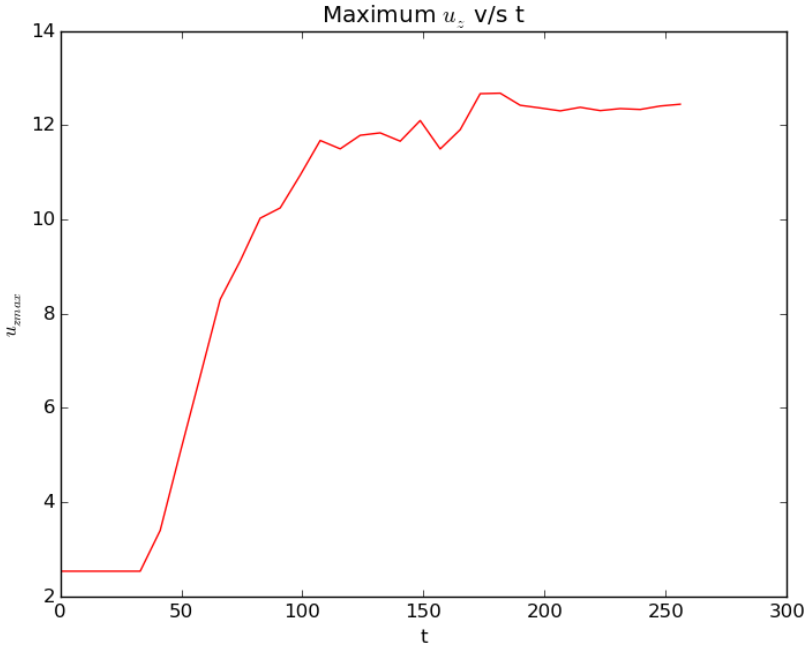


Figure 4.11: Maximum uz v/s t

Figure 4.12 shows the distribution function of uz in logarithmic scales. We can see that the distribution is broader than the initial velocity profile. This indicates the rise in temperature of electron.

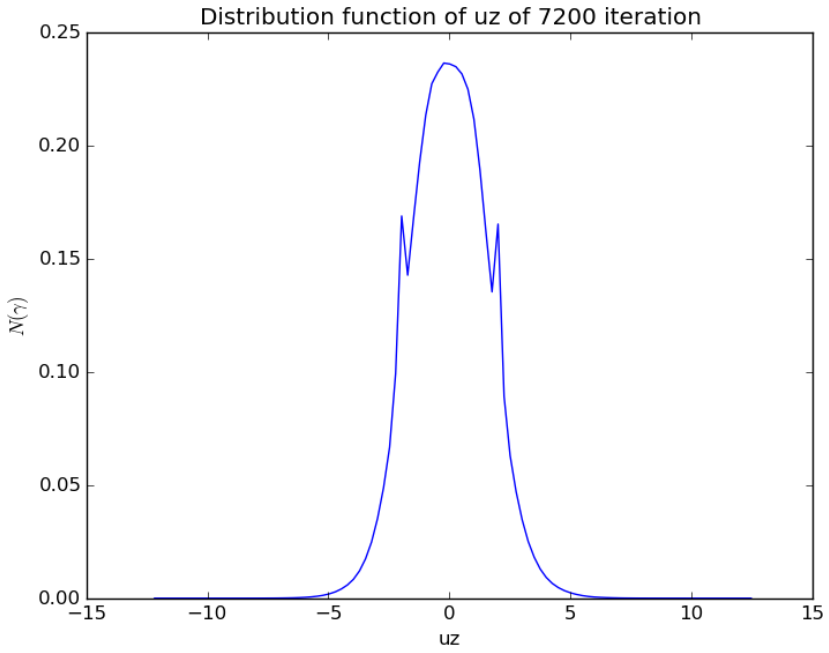


Figure 4.12: Distribution function of velocity

All the above results have been analysed for electrons. We see that the positrons also have the same features since their mass are equal to that of electron.

## 4.3 Conclusion

The simulation results clearly show that collisionless shocks can be driven in unmagnetized electron-positron plasmas. The structure of the collisionless shock propagates at an almost constant speed. We observe that after the shock more and more particles have higher velocities depicting the increase in temperature of the plasma, but there is a decrease in the bulk kinetic energy as most particles have zero $uz$. This dissipation of the upstream bulk kinetic energy is mainly due to the deflection of particles by the strong magnetic field generated around the shock transition region by the Weibel- type instability.

In the second part of project we would like to study shocks with already existing magnetic fields where we can observe particle acceleration, and study the mechanisms behind it.

# Bibliography


[1] A. R. Bell. The acceleration of cosmic rays in shock fronts – I. *Monthly Notices of the Royal Astonomical Society*, 182(2):147 – 156, 1978. doi: http://dx.doi.org/10.1093/mnras/182.2.147.

[2] Mikhail V. Medvedev and Abraham Loeb. Generation of Magnetic Fields in the Relativistic Shock of Gamma-Ray Burst Sources. *The Astrophysical Journal*, 526:697 – 706, 1999.

[3] Erich S. Weibel. Spontaneously Growing Transverse Waves in a Plasma Due to an Anisotropic Velocity Distribution. *Physics Review Letters*, 2:83, 1959. doi: http://dx.doi.org/10.1103/PhysRevLett.2.83.

[4] Tsunehiko N. Kato. RELATIVISTIC COLLISIONLESS SHOCKS IN UNMAGNETIZED ELECTRON-POSITRON PLASMAS. *The Astrophysical Journal*, 668:974–979, 2007.

[5] Scholarpedia J.M Laming. Collisionless Shocks, 2009. URL `http://www.scholarpedia.org/article/Collisionless_shock_wave`. [Online, accessed on 23-July-2015].

[6] Wikipedia. Weibel Instability — Wikipedia, The Free Encyclopedia, 2015. [Online, accessed on 23-November-2015].

[7] Burton D Fried. Mechanism for Instability of Transverse Plasma Waves.

[8] Warp project. URL `http://warpproject.org`.